Volumetric Interaction and Material Characterization of Flax/Furan Bio-composites

Jovana Džalto*, Luisa Medina, Peter Mitschang
Institut für Verbundwerkstoffe GmbH, Kaiserslautern, Germany

* Corresponding author. E-mail: jovana.dzalto@ivw.uni-kl.de
Received: 19 December 2013; Accepted: 27 January 2014; Published online: 13 February 2014
DOI: 10.14416/j.ijast.2014.01.004

Abstract
This paper deals with the characterization of a green composite, made of flax fibers and a bio-derived furan resin. It is shown that the porosity within the composite, which is determined by various parameters, adversely influences the mechanical performance as well as the water absorption behavior of the material. Since the furan resin induces a large amount of porosity during curing due to its foaming characteristic, the aim of this study is to find a method in order to minimize this so-called structural porosity. Therefore it is paid special attention to the conversion between weight and volume fractions and the volumetric interaction of the constituent phases. A model is applied in order to predict and minimize the porosity content in the composite.

Keywords*: Flax, Furan, Porosity, Biocomposite, Natural Fiber Textile*

1 Introduction

In recent years, natural fiber reinforced composites have gained much attention, both by academia and industry, due to their lightweight potential, low density, environmental performance and economic benefits [1]. A new and emerging area in polymer science is a specific class of bio-composites, where a bio-based polymer matrix is reinforced by natural fibers, the so-called green composites [2]. Due to increasing oil prices worldwide, the use of fully bio-based composites will probably be advantageous not only because of environmental reasons, but also from an economical viewpoint. In this context the usage of polylactide (PLA) as thermoplastic matrix is very promising, particularly with regard to the biodegradability of the biopolymer. Siengchin et al. [3] have shown that the mechanical performance of PLA is enhanced by reinforcing the matrix with woven flax fiber textiles. In addition the incorporation of alumina particles improves the physical behavior of the composite, but nevertheless the low thermal stability of PLA is still the limiting factor for the composite's applicability. On this account the presented work deals with the performance of a green composite made of woven flax fiber textiles and furan resin, which is derived from a waste product of the sugar production. Since most composite properties are directly influenced by the volume fraction of the constituents, and natural fibers are mostly indicated as weight fraction within the composite, the aim of this work is to apply a volumetric interaction model in order to facilitate the conversion between the constituents and hence, predict material properties. Due to the foaming characteristic of the furan resin the work does not only focus on the fiber and resin components of the composite, but also includes a third component, the porosity, which is assumed to highly determine the material properties.

2 Materials

The materials which are used within this work consist of a 3H satin weave flax textile as reinforcement and furan resin as matrix.

The high aligned flax fibers in the textile are entangled with polyester (PES) multi-filaments in order to ensure ideal coherence of the natural fibers during the weaving process (Figure 1). Another advantage of adding PES fibers into the composite structure is the possibility of improving the impact resistance of both thermoplastic and thermoset long natural fiber reinforced polymers [4].

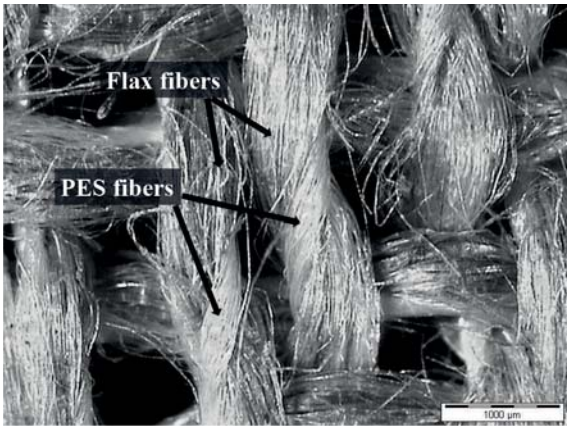

Figure 1: Flax textile with PES fibers.

The textile area weight is 420 g/m^2 and the PES fraction which is determined by separating and weighing the flax and synthetic fibers manually amounts to 18.5 wt.-%.

Furan resin is a thermoset polymer which is usually gained from renewable resources like bagasse, the waste product of the sugar production [5]. Therefore it is not in competition with the food industry.

The resin has been diluted with isopropyl alcohol in order to reduce the viscosity and facilitate a consistent textile impregnation. By storing the preimpregnated textiles - so-called prepregs - several days, most of the alcohol degassed from the system and afterwards the prepregs are manufactured to composite plates by compression molding. Two distance plates are inserted into the mold to define the height of the resulting laminates. The mold has to be lifted four times during compression so that the water resulting from the polycondensation of the furfuryl alcohol [6] evaporates (Figure 2). During the processing time of 480 s the mold temperature is approximately 150°C and the maximum pressure is 2 MPa. Seven plates with different fiber/resin weight fractions are produced using 3, 4, and 5 layers of prepregs. The plate volume in all cases is almost constant (450 × 320 × 2.45 mm^3) because of the foaming characteristic of furan resin and its ability to fill completely the predefined space in the mold. Thus, the produced plates have different porosity and fiber contents, which are controlled by the number of textile layers and the amount of resin.

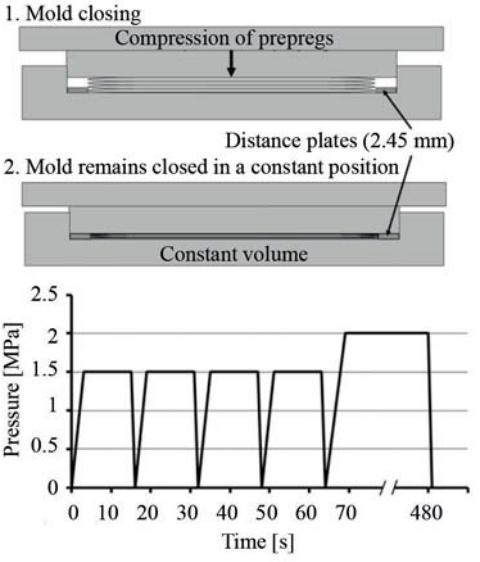

Figure 2: Schematic description of the compression molding with press cycle.

3 Methods

3.1 *Volumetric interaction*

The constant composite volume of the seven plates can be separated into a number of component volumes, i. e. fiber volume (v_f), matrix volume (v_m), and porosity volume (v_p). Minimizing the latter is the aim of this study and therefore it is paid special attention to porosity volumetric interaction. Flax fibers tend to absorb moisture from the atmosphere [7] which influences the mechanical properties of the composite [8]. The textile moisture content of approximately 5-8 wt.-% was measured in a previous work [9]. Nevertheless, the amount of water in the textile is not considered to be a volume component in the composite, because it is assumed that during compression molding the water either evaporates while the mold is opened or it induces composite porosity.

Madsen et al [10] describe the absolute volume of porosity (v_p) as sum of fiber correlated (v_{pf}), matrix correlated (v_{pm}), and structural porosity (v_{ps}).

$$v_p = v_{pf} + v_{pm} + v_{ps} \quad (1)$$

The fiber correlated porosity is determined by the cavities in the flax fibers (lumen), the porosity

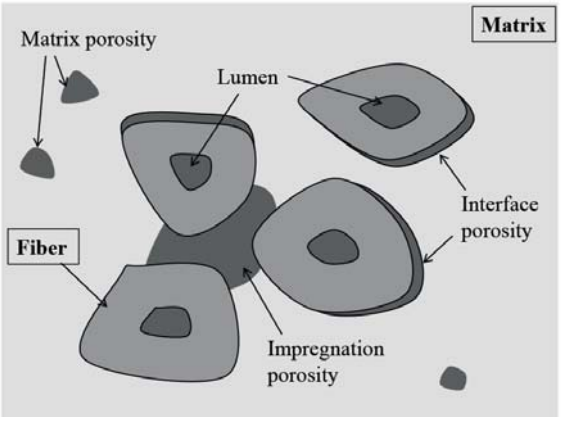

Figure 3: Schematic illustration of fiber porosity (v_{pf}) and matrix porosity(v_{pm}) [10].

due to insufficient fiber/matrix adhesion, and the porosity due to poor fiber impregnation. The voids in the matrix, which are identified to be air-filled cavities, are the matrix correlated porosity [10]. Both types of porosity can neither be influenced by optimizing the process nor by ideal fiber/matrix content in the composite, because they are assumed to be intrinsic material properties, which are linearly correlated with the absolute fiber and matrix volume. They are schematically described in Figure 3.

The porosity which can be minimized by the optimal combination of fiber and matrix weight fraction and the optimal process is the structural porosity which is mainly induced by the low packing ability of cellulose fibers [11] and in case of furan resin by the foaming characteristic of the matrix. It is assumed that the lower the amount of resin (at a given amount of textile layers), the more the resin is free to expand to fill the mold volume, and the higher is the resulting porosity content in the produced plates (Figure 4).

This means that the plate which consists of 3 prepreg layers should have the highest porosity content, whereas the plates which consist of 5 prepreg layers should have the lowest porosity content of the plates. In order to validate this assumption and to apply a model for conversion between the constituents, the volumetric interaction of the constituent volumes in the 7 plates can be quantified as follows. The weight fraction of the textile $\psi_{textile}$ is measured by the ratio of the area weight of the composite plates $AW_{composite}$ and the area weight of

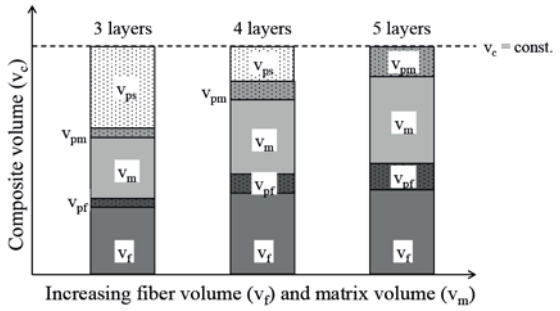

Figure 4: Schematic illustration of reducing structural porosity (v_{ps}).

the applied textile layers $AW_{textile\ layers}$ (equation (2)). Since the air-filled voids do not contribute to the composite weight, the weight fraction of the resin ψ_{resin} is the remaining weight fraction in the composite (equation (3)).

$$\psi_{textile} = \frac{AW_{textile\ layers}}{AW_{composite}} \tag{2}$$

$$\psi_{resin} = 1 - \psi_{textile} \tag{3}$$

The volume fraction of the textile $\varphi_{textile}$ as well as the volume fraction of the resin φ_{resin} can be calculated as shown in equations (4) and (5) [12].

$$\varphi_{textile} = \frac{\rho_{composite}}{\rho_{textile}} \cdot \psi_{textile} \tag{4}$$

$$\varphi_{resin} = \frac{\rho_{composite}}{\rho_{furan}} \cdot \psi_{resin} \tag{5}$$

$\rho_{composite}$ is the density of the composite and it is determined in each plate by the ratio of the composite plate and its volume. The density of the total cured furan resin ρ_{furan} was measured in a previous work as 1.334 g/cm^3 [13]. The density of the textile $\rho_{textile}$ can be calculated according to the linear mixing rule with the textile weight fraction (18.5 wt.-%) and density of PES fibers ρ_{PES} = 1.415 g/cm^3 (measured by project partner Riso DTU, Denmark) and the weight fraction and density of flax fibers ρ_{flax} = 1.5 g/cm^3 [14] as shown in equation (6).

$$\rho_{textile} = 0.185 \cdot \rho_{PES} + (1 - 0.185) \cdot \rho_{flax} = \\ = 1.48\ \text{g/cm}^3 \tag{6}$$

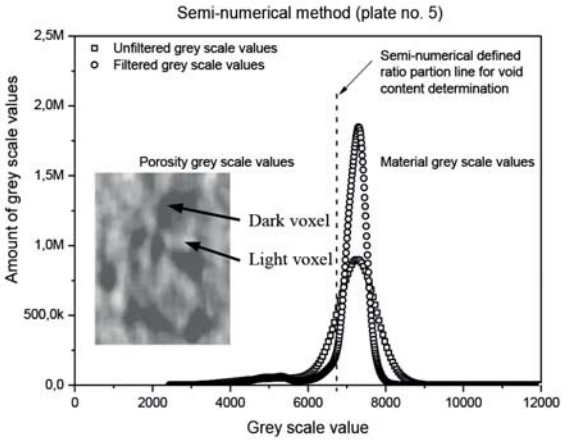

Figure 5: Histogram of plate 5 using the semi-numerical method with grey scale image.

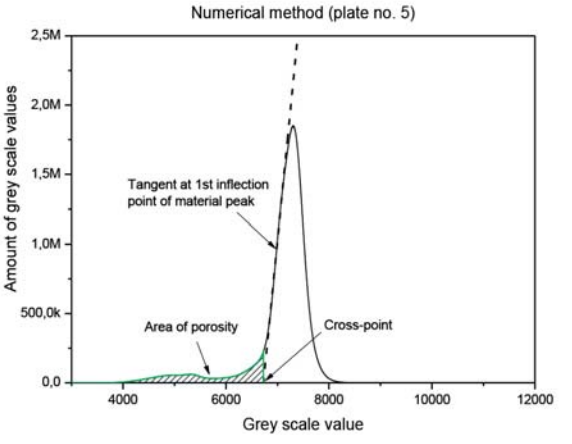

Figure 6: Histogram of plate 5 using the numerical method.

Although the porosity in the composite does not contribute to the weight fraction, the voids still have a measurable volume fraction φ_{poro}. It is the remaining volume fraction in the composite as shown in equation (7).

$$\varphi_{poro} = 1 - (\varphi_{textile} + \varphi_{resin}) \quad (7)$$

3.2 *Model validation via porosity content measurements by µCT*

In chapter 3.1 the porosity is determined by calculating the volume fractions of the constituent phases. In order to validate this gravimetric method the porosity of the seven plates is measured with a 3D computed micro-tomography system (µCT) from Phoenix x-ray systems + services GmbH. For this purpose so-called target objects with a size of 2 mm × 2 mm × 4 mm are taken out from every above-mentioned plate. The objects are x-rayed from two different directions in order to create a virtual 3D model of every sample. Using the visualization software Volume Graphics Studio Max the collected pixels are summarized to voxels whereas every voxel represents a 3D information unit. The total amount of voxels (here: 1,024,000,000 voxels) represents the whole 3D image whereas every voxel of this image consists of a greyscale value. If a voxel consists of different materials with different densities, the Partial Volume Effect occurs, i.e. the appearing signal is a mean value of different material components [15, 16]. The greyscale values represent the different densities within the target objects. Black and dark greyscale values are materials with low density, respectively air. Materials with higher densities possess light grey tones. The analyzed grey scale values are summarized in histograms.

Two different analysis methods are used to determine the porosity of the materials, the semi-numerical method as well as the numerical method. In both methods a smoothing filter is applied to illustrate the separation between porosity and material.

Figure 5 shows exemplary the histogram of plate no. 5 and it can be observed that the curve possesses only two peaks. Since the densities of flax and PES fibers as well as the density of furan resin are very similar compared to the density of air (~ 1,2 · 10-3 g/cm^3) the great peak represents the fibers and the resin whereas the small peak represents air, respectively porosity. The area below the filtered curve determines the volume ratio of both, porosity and material. With the semi-numerical method the grey scale image is used in order to decide if a pixel belongs to porosity or to material. This method is also known as region of interest analysis (ROI) [17].

In contrast to the semi-numerical method, the numerical method considers only the frequency distribution of the curve without taking the grey scale images into account [17]. Figure 6 shows the numerical analysis of the histogram of plate no. 5. In order to determine the transition zone between porosity and material area under the curve a tangent

Table 1: Weight and volume fractions of the manufactured composite plates

Composite plate no. [-]	Amount of layers [-]	Composite density [g/cm³]	$\psi_{textile}$ [wt.-%]	ψ_{resin} [wt.-%]	$\varphi_{textile}$ [vol.-%]	φ_{resin} [vol.-%]	φ_{poro} [vol.-%]
1	3	1.02	52.35	47.65	36.23	36.70	27.07
2	4	1.16	61.89	38.11	48.51	33.24	18.25
3	4	1.33	53.23	46.77	47.70	46.63	5.67
4	4	1.23	59.19	40.81	49.35	37.86	12.78
5	4	1.30	54.80	45.20	48.30	44.34	7.36
6	5	1.40	62.15	37.85	58.88	39.91	1.22
7	5	1.32	65.38	34.62	58.15	34.27	7.58

is applied at the first inflection point of the material peak. The cross-point of this tangent and the axis of abscissae is seen as the transition point, which means that the area to the left of the cross-point represents the porosity volume ratio and the area to the right of the point represents the material volume ratio.

3.3 *Water absorption properties*

Since flax fibers are derived from lignocellulose which contains polarized hydroxyl groups, the hydrophilic nature of the fibers is one of the major disadvantages of flax fiber composites because the fibers tend to absorb water and to swell [14]. This can lead to a decreasing mechanical performance of the composite [18]. In order to prove if the water absorption is also adversely influenced by the porosity content the water uptake behavior of the produced plates is analyzed whereas from every plate 5 specimens are cut out with the dimensions of 50 mm × 50 mm. The specimens are vertically placed into a water basin in order to ensure water contact to the exposed fibers at the cut edges as well as the areas without exposed fibers at the top and bottom of the specimens. After 24 h, 96 h, 192 h, and 380 h the specimen weight is measured and compared to the initial weight of the dry specimens. After 380 h the long-term test has been stopped since most of the specimens almost reached equilibrium. The water uptake ψ_{Water} in wt.-% is calculated using equation (8) in which m_t is the specimen weight at time t (24-380 h) and m_0 is the initial weight at time 0.

$$\psi_{Water} = \frac{m_t - m_0}{m_0} \cdot 100 \qquad (8)$$

3.4 *Mechanical properties*

Tensile properties are measured according to DIN EN ISO 527-4 on a Zwick universal testing machine (specimen size for type 2 specimens: 250 mm × 25 mm), and Charpy impact resistance tests according to DIN EN ISO 179 with unnotched specimens (specimen size for type 2 specimens: 80 mm × 15 mm, span L = 20 × thickness) are carried out with the above-mentioned plates.

4 Results and Discussion

4.1 *Results of the volumetric interaction*

In this study 7 composite plates are manufactured with textile weight fractions in the range 52-65% which are determined by the amount of prepregs layers (3, 4, and 5 layers). Using the above-mentioned equations with regard to the porosity content and constituent volume fractions, the results of the determined volumetric composition of the manufactured 7 plates are presented in Table 1.

It shows three groups of composites with almost constant textile volume fractions $\varphi_{textile}$ of 0.36, 0.48 and 0.58, which correspond to the 3, 4 and 5 layers of textile, respectively, used in the manufacturing process. A standard deviation cannot be specified because only one plate was produced for each specified textile volume fraction. The porosity values of the manufactured composites are in the range 1.22-27.07%. Due to the constant mold volume the obtained textile volume is directly correlated with the number of textile layers. It can be observed that within each group of constant $\varphi_{textile}$

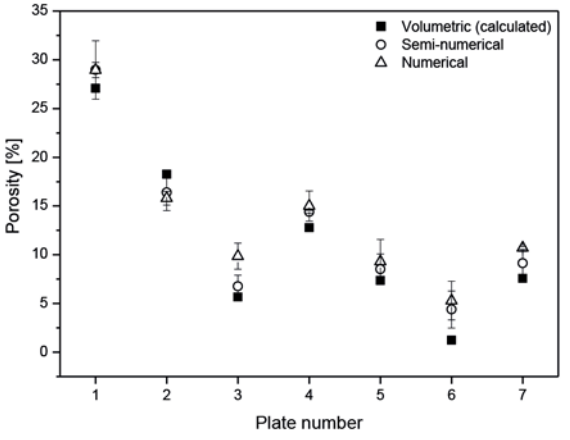

Figure 7: Comparison between calculated (volumetric), semi-numerically and numerically determined porosity.

the porosity content φ_{poro} increases consistently with increasing textile weight fraction $\psi_{textile}$ or analogously with decreasing resin weight fraction ψ_{resin}. In order to predict the required weight fractions of textile and resin for producing low porosity composites a model is needed for the exact numerical relation between weight and volume fractions of the constituents.

4.2 *Comparison with µCT*

In order to examine the applicability of the volumetric composition, the porosity values from Table 1 are compared to the results of the µCT analysis. The comparison of the results of the ROI and the numerical method with the volumetrically calculated porosity is shown in Figure 7.

Both methods are representing the volumetric porosity very well. Except in plate no. 2 the calculated porosities are lower than the measured porosities whereas in all cases the porosity values of the semi-numerical method are closer to the calculated values. The reason for the deviations between calculated and measured porosities can be the very small sample size of the target objects, which is not representative for the entire plate. Another reason could also be the inhomogeneous distribution of the furan resin along the plates, resulting from insufficient fiber impregnation. In [10] it is reported that in some cases the polymer matrix is able to diffuse into the lumen of the fibers due to large openings in the cell walls of the fibers. By eliminating the porosity which is located

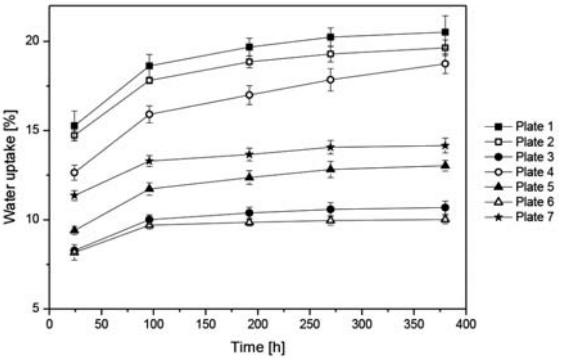

Figure 8: Weight increase of the specimens between 0 h and 380 h.

inside the fibers, this effect can also influence the porosity content of natural fiber composites. However, the porosity measurements validate the volumetric calculation method of the constituents, because the distinctions of the values are in an acceptable range.

4.3 *Water absorption properties*

In Figure 8 it can be observed that after 24 hours the water uptake of the 7 composite plates is in the range 8% - 15% compared to the initial weight of the dry specimens. After 380 hours the test is stopped because the water uptake of the 7 produced plates reaches a near-equilibrium state and the weight of the specimens does not show any further increase (the average weight gain from 270 to 380 hours is 1.7%). Since the difference in water uptake after 380 h is more pronounced than after 24 h these values have been used for the following charts. Nevertheless, the qualitative statement remains the same.

Due to the hydrophilic behavior of bast fibers the first expectation is that the water uptake is mainly determined by the weight content of the flax fibers, but this assumption cannot be validated in this case (Figure 9). Surprisingly, there is no correlation between water absorption after 380 hours and fiber weight fraction. However, it can be observed a correlation between water uptake and porosity content (Figure 10). The higher the porosity content within the plate the higher is the water uptake after 380 hours. Therefore the composite plate 6 with the lowest porosity content has only a water uptake of 10% after 380 h. Plate 1 with the highest porosity content has a water uptake of 20.5% which is twice as high,

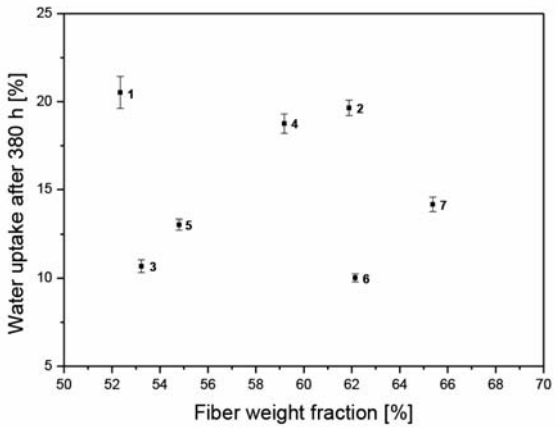

Figure 9: Water uptake in relation to fiber weight fraction.

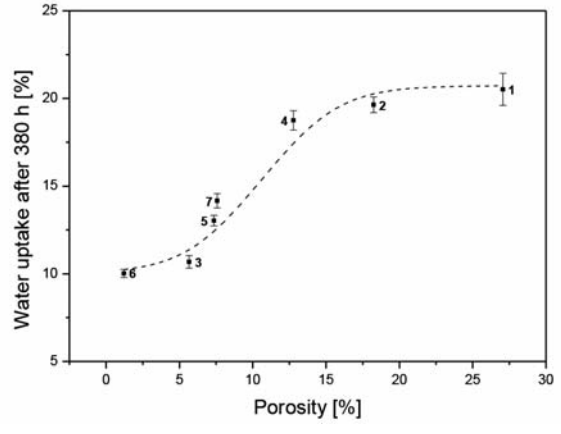

Figure 10: Water uptake in relation to porosity.

although this is the plate with the lowest fiber weight fraction. A reason for the correlation between porosity and water uptake can be seen in the surface structure of the specimens, which is observed using an optical microscope (Figure 11).

Specimens with high porosity content show pores with larger mean diameter at their surface. Specimens with low porosity content have a much smoother surface with a glossy surface finish with smaller diameter pinholes. Considering that the specimen surface is completely covered with water during the absorption test it is obvious that the water has an easier way to diffuse through the larger pores than through the pores with small diameter. Hence, the probability of water uptake on the part of hydrophilic flax fibers is higher for composites with high porosity content due to the porous surface structure.

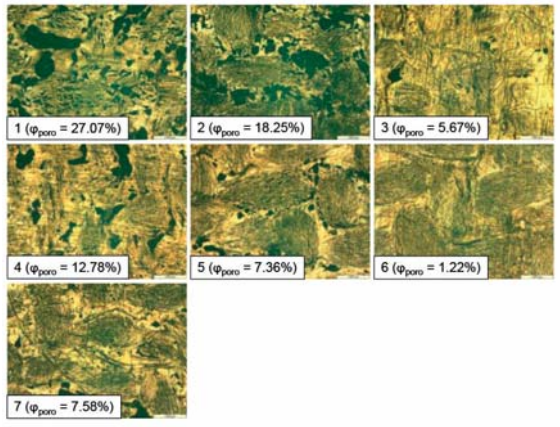

Figure 11: Surface structure of the composites.

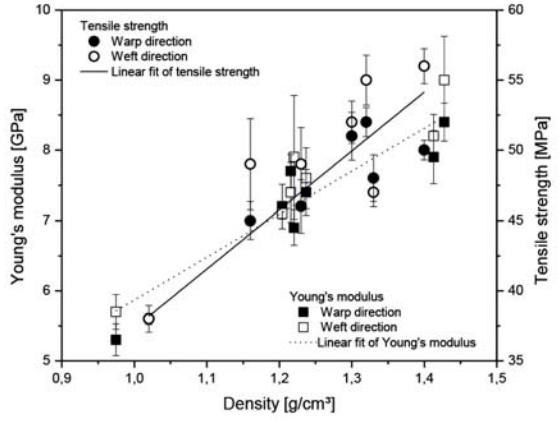

Figure 12: Young's modulus in relation to the composite density.

4.4 *Mechanical properties*

The tensile composite properties are measured in the range 5-9 GPa for stiffness and 38-56 MPa for strength in both, the warp and weft direction of the textile. The impact resistance for unnotched specimens is measured in the range 9-28 kJ/m^2 also in warp and weft direction.

As might be expected, the stiffness and strength clearly correlate with the composite density (Figure 12), which is in fact determined by the porosity content. On that account the Young's modulus as well as the tensile strength are mainly influenced by the porosity content, i.e. the values increase with decreasing porosity (Figure 13). Although stiffness and impact strength are contradictory material properties [4], Figure 13 also shows increasing

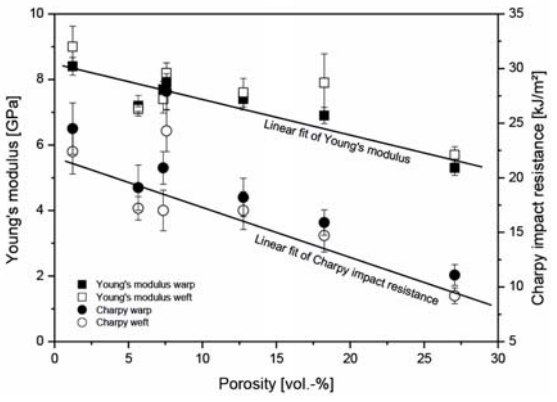

Figure 13: Young's modulus and Charpy impact resistance in relation to the density.

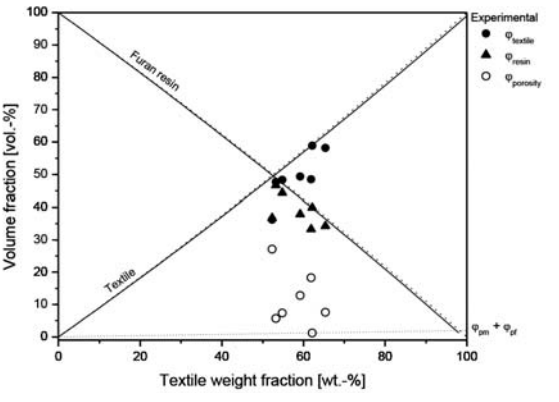

Figure 14: Composite volumetric interaction without considering structural porosity compared to experimentally gained values.

impact resistance with decreasing porosity. It can be noted that the linear fit curves of Young's modulus as well as Charpy impact resistance are strictly monotonic decreasing with increasing porosity volume content.

The explanation for this behavior is based on a theoretical study of MacKenzie [19], which asserts that material stiffness is adversely influenced by adding spherical holes, i.e. porosity, into the material, because the holes introduce stress concentrations into the material [20].

4.5 *Composite volumetric interaction*

Since most composite properties are directly influenced by the volume and not by the weight of the reinforcing fibers [20], there is a need to convert fiber weight fraction into fiber volume fraction. Within an ideal composite without porosity the volume fractions of the constituents, i.e. resin φ_{resin} and textile $\varphi_{textile}$, can be calculated according to equation (9) and (10).

$$\varphi_{resin} = \frac{v_{resin}}{v_{composite}} = \frac{\frac{\psi_{resin}}{\rho_{resin}}}{\frac{\psi_{textile}}{\rho_{textile}} + \frac{\psi_{resin}}{\rho_{resin}}} \tag{9}$$

$$\varphi_{textile} = \frac{v_{textile}}{v_{composite}} = \frac{\frac{\psi_{textile}}{\rho_{textile}}}{\frac{\psi_{textile}}{\rho_{textile}} + \frac{\psi_{resin}}{\rho_{resin}}} \tag{10}$$

In Figure 14 the numerical outcome of this simple model (dotted lines for furan and textile volume fraction) is plotted as a function of textile weight fraction ($\psi_{textile}$) together with the experimentally gained values for textile, resin, and porosity weight fraction. A standard deviation cannot be specified for the experimental data because only one plate was produced for each specified textile weight fraction.

It is assumed that in plate 6 with a calculated porosity content of 1.22 vol.-% the fibers are fully compacted to their minimum volume and that the furan resin is just sufficient to fill the free mold space. Hence, the calculated porosity volume is composed of matrix correlated φ_{pm} and fiber correlated porosity φ_{pf} and does not contain any structural porosity φ_{ps} (equation (11)).

$$\varphi_p = \varphi_{pm} + \varphi_{pf} \quad , \quad \varphi_{ps} = 0 \tag{11}$$

Mathematically, the matrix and fiber correlated porosity within the composite can then be described as a linear function, which increases with increasing textile weight fraction, whereas the slope of the line can be easily calculated with the coordinates of the porosity of 1.22 vol.-% in Figure 14. Equation (12) is the linear equation of the line, which can also be seen as dotted line in Figure 14.

$$f(x) = \frac{1.22}{62.15} \cdot x = 0.0196 \cdot x \quad , \tag{12}$$

$$f(x)\ domain = [0,100]$$

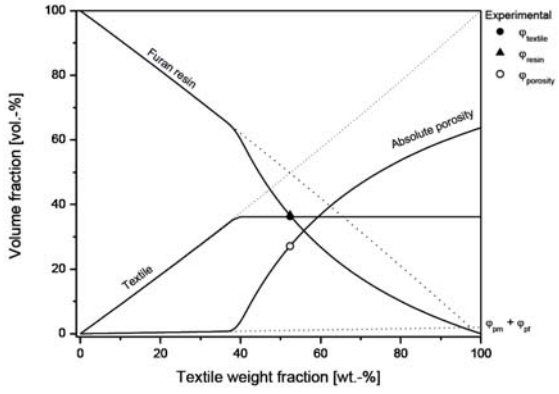

Figure 15: Volumetric interaction with 3 textile layers.

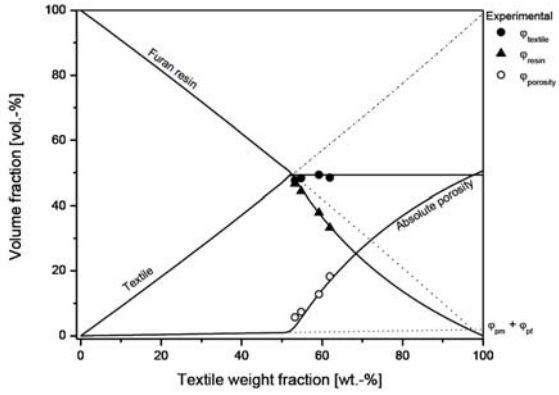

Figure 16: Volumetric interaction with 4 textile layers.

For the identification and quantification of porosity sub-components [10] gives a useful overview, but in this case it is not possible to establish in which proportion the porosity is divided into matrix and fiber correlated porosity, because of the lack of microscope cross-sectional observations for the produced plates. Therefore, a gross assumption is made, concerning that half of the porosity is fiber correlated and the other half is matrix correlated porosity. The expanded model with consideration of the porosity can also be seen in Figure 14 as continuous lines for resin and textile volume fractions.

Both models shown in Figure 14 do not fit the experimental data for textile, resin and porosity volume fractions very well, because the structural porosity within the composites is not taken into account. With the above-mentioned model the values cannot be calculated neither for the textile nor the resin nor the porosity volume content.

On this account a volumetric interaction model is used, which has been developed by Madsen et al [10, 20, 21] in order to facilitate the prediction of the constituent volume fractions for flax/furan composites with constant volumes, but different amounts of textile layers. Madsen implies that an optimal combination of high fiber content and low porosity content exists, which is known as transition case. The transition fiber volume fraction $\varphi_{f\,trans}$ is equal to a maximum achievable fiber weight fraction, which in this case is the maximum achievable textile volume fraction $\varphi_{textile\,max}$. These maximum achievable volume fractions for 3, 4, and 5 layers of textile within the manufactured composites are gathered from table 1. The corresponding values for textile volume fractions are 36.2 vol.-% for 3 layers, 49.4 vol.-% for 4 layers, and 58.9 vol.-% for 5 layers of flax textile. After reaching these volume fractions a volume of structural porosity φ_{ps} occurs, which has to be added to the matrix and fiber correlated porosity and deducted from the resin volume fraction. Therefore, the associated values for resin and structural porosity volume fractions (φ_{resin} and φ_{ps}) are calculated according to equations (13) and (14) [10].

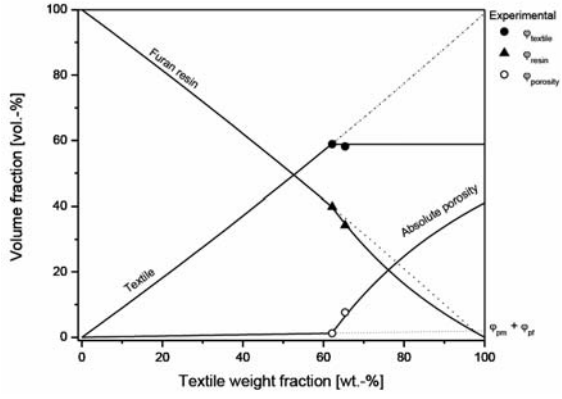

Figure 17: Volumetric interaction with 5 textile layers.

$$\varphi_{resin} = \frac{\varphi_{textile\,max} \cdot \psi_{resin} \cdot \rho_{textile}}{\psi_{textile} \cdot \rho_{resin}} \quad (13)$$

$$\varphi_{ps} = 100 - (\varphi_{resin} + \varphi_{textile\,max}) \quad (14)$$

The expanded model with consideration of structural porosity and experimental values for 3 textile flax layers can be seen in Figure 15, for 4 layers in Figure 16, and for 5 layers in Figure 17.

It is obvious that this model describes the volumetric interaction much better. Through the fact that for the example of 3 layers only one composite is considered, the model cannot be validated under consideration of other experimentally gained data.

The curves for 4 and 5 layers fit the experimental data very well. It can be observed that the porosity volume fraction for low textile weight fractions is monotonically increasing and that the porosity is the result of fiber and matrix correlated porosity. At higher textile weight fractions the textile volume fraction is constant whereas the porosity increases strongly without reference to the textile layers. Consequently the resin volume fraction starts to decrease with increasing porosity content. The point where the structural porosity starts to increase determines the optimal combination of high fiber content and low porosity content. Madsen et al call it the transition case [10]. It can be gained from the diagrams that for 3 textile layers the transition fiber weight fraction is $\psi_{f3\ trans}$ = 40%, for 4 textile layers $\psi_{f4\ trans}$ = 52%, and for 5 textile layers $\psi f_{5\ trans}$ = 62% and that these fiber weight fractions are characterized by the optimal combination of high textile volume fraction and low porosity, which leads to a better mechanical performance of the composite. The model is a helpful tool for understanding the fundamental interaction between natural fibers and furan resin and for optimizing the manufacturing process towards high performance composites with high density.

5 Conclusions

Within this work bio-composites, composed of flax textile and furan resin, are fabricated with constant volume, but different textile and resin fractions, which are determined by the amount of flax textile layers. The porosity within the fabricated composites has a significant and negative influence on the material performance, i.e. water absorption and mechanical properties, such as stiffness and strength as well as the impact resistance. Minimizing the porosity, which is caused by different factors like the low packaging ability of flax fibers and the foaming behavior of furan resin, has therefore a great importance. Knowledge of the interaction between volume fractions of textile, resin and porosity is essential with respect to optimize the material performance. The volumetric interaction model, which is developed by Madsen et al, provides a suitable tool to predict the volume fractions of the constituents. In order to validate and optimize the model for flax/furan bio-composites, there is a need for more experimental data. Therefore, the aim of future work is to prove if there are additional volumetric interactions, which are not considered in this work. Several assumptions are made in order to simplify the model, which could have a potential influence of the volumetric interaction. One assumption is the density of the flax fibers, which is not established in this work. Since the lumen of the fibers is part of the fiber correlated porosity in the composite, it is possible that the density without consideration of the lumen is much higher than the assumed flax fiber density in this work. Also the water content of the fibers and the water resulting from the polycondensation of furfuryl alcohol is neglected, although the fabricated composites have a residual moisture inside their structure, which can be measured after drying the just fabricated specimens. For this reason the aim of future work is to expand the volumetric interaction model to include a fourth component, the water. For a more precise consideration of the proportion of fiber and matrix correlated porosity light microscope images can also be taken into account.

Acknowledgements

The research leading to these results has received funding from the European Community's Seventh Framework Programme (FP7/2007-2013) under grant agreement n° 214467 (NATEX).

References

[1] H. L. Bos, J. Müssig, and M. J. A. van den Oever, "Mechanical properties of short-flax fibre reinforced compounds," *Composites Part A*, vol. 37(10), pp. 1591-1604, 2006.

[2] E. Zini and M. Scandola, "Green Composites: An Overview," *Polymer Composites*, vol. 32(12), pp. 1905-1915, 2011.

[3] S. Siengchin, T. Pohl, L. Medina, and P. Mitschang, "Structure and properties of flax/polylactide/alumina nanocomposites," *Journal of Reinforced Plastics and Composites*, vol. 32(1), pp. 23-33, 2013.

[4] T. Reußmann, K.-P. Mieck, and R. Lützkendorf, "Möglichkeiten der Schlagzähmodifizierung thermo-

und duroplastischer Natur-Langfaserverbunde," presented at the 4th International Wood and Natural Fibre Composites Symposium, Kassel, Germany, Apr. 10-11, 2002.

[5] A. Gandini, "Polymers from Renewable Resources: A Challenge for the Future of Macromolecular Materials," *Macromolecules*, vol. 41(24), pp. 9491-9504, 2008.

[6] S. S. Oishi, M. C. Rezende, F. D. Origo, A. J. Damião, and E. C. Botelho, "Viscosity, pH, and moisture effect in the porosity of poly(furfuryl alcohol)," *Journal of Applied Polymer Science*, vol. 128(3), pp. 1680-1686, 2013.

[7] A. Bismarck, I. Aranberri-Askarogorta, and J. Springer, "Surface Characterization of Flax, Hemp and Cellulose Fibers; Surface Properties and the Water Uptake Behavior," *Polymer Composites*, vol. 23(5), pp. 872-894, 2002.

[8] J. K. Pandey, S. H. Ahn, C. S. Lee, A. K. Mohanty, and M. Misra "Recent Advances in the Application of Natural Fiber Based Composites," *Macromolecular Materials and Engineering*, vol. 295(11), pp. 975-989, 2010.

[9] M. Bierer, T. Pohl, E. Natter, B. Madsen, H. Hoydonckx, and R. Schledjewski, "Properties of new fully bio-based thermoset composites," presented at the 14th European Conference on Composite Materials, Budapest, Hungary, Jun. 7-10, 2010.

[10] B. Madsen, A. Thygesen, and H. Lilholt, "Plant fibre composites-porosity and volumetric interaction," *Composites Science and Technology*, vol. 67(7-8), pp. 1584-1600, 2007.

[11] CELC European Scientific Committee, *Flax and Hemp fibres: a natural solution for the composite industry*, Paris: JEC, 2012.

[12] H. Schürmann, *Konstruieren mit Faser-Kunststoff Verbunden*, Springer-Verlag, Berlin Heidelberg: 2008.

[13] T. Pohl, M. Bierer, E. Natter, B. Madsen, H. Hoydonckx, and R. Schledjewski, "Properties of compression moulded new fully biobased thermoset composites with aligned flax fibre textiles," *Plastics, Rubber and Composites*, vol. 40(6-7), pp. 294-299, 2011.

[14] M. J. John and R. D. Anandjiwala, "Recent Developments in Chemical Modification and Characterization of Natural Fiber-Reinforced Composites," *Polymer Composites*, vol. 29(2), pp. 187-207, 2008.

[15] M. A. Gonzales Ballester, A. P. Zisserman, and M. Brady, "Estimation of the partial volume effect in MRI," *Medical Image Analysis*, vol. 6(4), pp. 389-405, 2002.

[16] R. Schmitt and U. Lanz, "Bildgebende Diagnostik der Hand," in *Georg Thieme Verlag*, Stuttgart, 2004.

[17] L. G. Astrakas and M. I. Argyropoulou, "Shifting from region of interest (ROI) to voxel-based analysis in human brain mapping," *Pediatric Radiology*, vol. 40(12), pp. 1857-1867, 2010.

[18] S. Kalia, B. S. Kaith, and I. Kaur, "Pretreatments of Natural Fibers and their Application as Reinforcing Material in Polymer Composites-A Review," *Polymer Engineering and Science*, vol. 49(7), pp. 1253-1272, 2009.

[19] J. K. MacKenzie, "The Elastic Constants of a Solid containing Sperical Holes," in *Proceedings of the Physical Society, section B*, 1950. vol. 63(1), pp. 2-11.

[20] B. Madsen and H. Lilholt, "Physical and mechanical properties of unidirectional plant fibre composites-an evaluation of the influence of porosity," *Composites Science and Technology*, vol. 63(9), pp. 1265-1272, 2003.

[21] B. Madsen, A. Thygesen, and H. Lilholt, "Plant fibre composites-porosity and stiffness," *Composites Science and Technology*, vol. 69(7-8), pp. 1057-1069, 2009.